Journal of Microbiological Methods 120 (2016) 34–40

Contents lists available at ScienceDirect

Journal of Microbiological Methods

journal homepage: www.elsevier.com/locate/jmicmeth

Three supplementary methods for analyzing cytotoxicity of *Escherichia coli* O157:H7

Xin Zhang [a,b,1], Yuxia Li [a,1], Bingjuan Li [a], Yan Mao [a], Xun Wu [a], Xiaohua Zou [a], Peng Gao [a,b], Hexin Yan [a], Dan Yang [a], Yan Ling [a,*], Huipeng Chen [a,*]

[a] Beijing Institute of Biotechnology, Beijing 100071, China
[b] School of Life Sciences, Anhui University, Hefei 230601, Anhui, China

ARTICLE INFO

Article history:
Received 14 April 2015
Received in revised form 13 November 2015
Accepted 14 November 2015
Available online 17 November 2015

Keywords:
EHEC
O157:H7
Pathogenicity
Virulence
Cytotoxicity

ABSTRACT

Escherichia coli O157:H7 is an enterohemorrhagic *E. coli* (EHEC) strain and a major food-borne pathogen, causing severe disease in humans worldwide. Multiple sensitive, accurate, and quantitative methods are needed to provide a comprehensive analysis of cell damage caused by O157:H7. However, the current, universally adopted methods for O157:H7 virulence assessment fail to investigate the interactive effects of O157:H7 and its host cells, neglect the effects of infection of host cells by O157:H7, and fail to comprehensively and accurately reflect the true pathogenicity of O157:H7. In this study, three different accurate, sensitive, and quantifiable methods were supplementary to provide standard operating procedures to analyze the cytotoxicity of O157:H7. This set of methods can be applied to toxicity studies of newly discovered O157:H7 clinical isolates and used to study how a clinical isolate's toxicity correlates with its pathogenicity. These methods can also be used in future studies of latent virulence factors and to explore the pathogenic mechanisms of O157:H7.

© 2015 The Authors. Published by Elsevier B.V. This is an open access article under the CC BY-NC-ND license (http://creativecommons.org/licenses/by-nc-nd/4.0/).

1. Introduction

Since 1982, when the first *Escherichia coli* O157:H7-induced food poisoning outbreak occurred in the U.S., O157:H7 epidemics have gradually proliferated and spread in many areas around the world (Beltz, 2011; Lynch et al., 2006). In China, reported cases of O157:H7 infections occur each year. In 1999, a particularly severe O157:H7 infectious diarrheal epidemic occurred in Jiangsu and other areas, with as many as 20,000 affected patients.

E. coli O157:H7 is an enterohemorrhagic *E. coli* (EHEC) strain and a major food-borne pathogen, causing severe diseases in humans worldwide. O157:H7 infections result mainly from the ingestion of contaminated food or water or from oral contact with contaminated surfaces (Mead and Griffin, 1998). The toxicity of O157:H7 is very high (Kauffman and LeJeune, 2011), and the minimum infectious dose is less than 10 pathogenic bacteria (Garg et al., 2008). Moreover, this pathogen may be highly lethal. The O157:H7 strain infection may be asymptomatic, or it may induce clinical symptoms including mild diarrhea, hemorrhagic enteritis, hemolytic–uremic syndrome sace (Niles et al., 2007), and thrombotic thrombocytopenic purpura (TTP) (Byelashov et al., 2010). Antibiotic treatment can lead to aggravation of the O157:H7 infection (Bielaszewska et al., 2011), but the exact etiology of this phenomenon remains unclear. Currently, there are no efficacious treatments for O157:H7 infection.

The O157:H7 genome harbors three major virulence loci, namely the locus of enterocyte effacement (LEE) pathogenicity island (Wong et al., 2011), the Shiga toxin (Stx) prophage, and the F-like plasmid pO157 (Perna et al., 2001; Hayashi et al., 2001). The LEE pathogenicity island encodes a type III secretion system that is able to secrete effector proteins out of bacterial cells and deliver them into host cells, which not only induces the attaching and effacing lesions but also subverts multiple host cell signaling pathways during infection. The Stx prophage encodes Stx1 and Stx2, which are antigenically distinct toxins with similar biological activities of cell damage (Strockbine et al., 1986). The pO157 plasmid encodes a number of virulence factors, including the enterohemolysin EhxA, the secreted serine protease EspP, the catalase–peroxidase KatP, the adhesin ToxB, the Cl esterase inhibitor StcE, and the type II secretion system (Lim et al., 2010). Nevertheless, the detailed roles of these virulence factors in the pathogenicity of O157:H7 are largely unknown, and there may be additional, uncharacterized virulence factors.

* Corresponding authors.
E-mail addresses: lingyanbeijing@163.com (Y. Ling), chenhp0909@163.com (H. Chen).
[1] Xin Zhang and Yuxia Li contributed equally to this work.

http://dx.doi.org/10.1016/j.mimet.2015.11.011
0167-7012/© 2015 The Authors. Published by Elsevier B.V. This is an open access article under the CC BY-NC-ND license (http://creativecommons.org/licenses/by-nc-nd/4.0/).

Multiple virulence factors, including those encoded by the above three virulence loci, are involved in the bacterial toxicity against host cells (Moxley, 2004; Wang et al., 2011; Dziva et al., 2007), which is a major component of O157:H7 pathogenicity. Analyzing bacterial cytotoxicity is clearly important for the virulence assessment of O157:H7.

The pathogenicity of O157:H7 is closely related to its toxicity to host cells, and the level of O157:H7 toxicity depends on the strength of the effects of its virulence factors. The interaction between the organism's virulence factors and the cellular target site forms the molecular basis for O157:H7 infection and pathogenicity.

After O157:H7 infects the epithelial cells of the host digestive system, it induces cytotoxicity by interacting with the intestinal epithelial cells (Bielaszewska et al., 2011). The virulence associated with this interaction is used to determine the level of toxicity (Moxley, 2004).

At present, functional studies of the known O157:H7 virulence factors are insufficient. Efforts to understand the mechanisms of interaction between the virulence factors and the host remain unsystematic. Furthermore, the pathogenic mechanism of O157:H7 has not been comprehensively clarified. As a result, the virulence assessment is very important for analyzing the cytotoxicity of O157:H7. Virulence involves quantitative concepts. To analyze the cytotoxicity of O157:H7, it is necessary to employ quantifiable virulence assessment methods with a defined sensitivity. The virulence of O157:H7 for host cells is composed of many factors. The O157:H7 chromosome encodes at least 131 proteins assumed to have virulence-related functions that are not present in the K-12 strain (Shabanova et al., 2009). The superposition of effects of the various O157:H7 virulence factors on the host cells determines the level of virulence. Therefore, investigating only one or a few of the existing virulence factors of O157:H7 and their effects may not reflect the actual toxicity of O157:H7.

Currently, the widely adopted methods for virulence assessment of O157:H7 primarily include gene detection (Hayashi et al., 2001) (polymerase chain reaction (Lebeis et al., 2008) and blotting techniques), Shiga-like toxin (SLT) detection (Bonetta et al., 2011), and testing for attachment and effacing damage (A/E damage) (Badouei et al., 2010). The genetic analysis of a sample can only provide information on gene sequences; it cannot demonstrate virulence factor expression. SLT detection only investigates the cytotoxicity effects of some virulence factors of O157:H7; it does not reflect the full toxicity of O157:H7. Testing for A/E damage mainly focuses on analyzing the interaction between O157:H7 and the host cell skeletal molecule F-actin, neither providing an accurate quantification of the damage nor assessing the full cytotoxicity effects of O157:H7 infection. Finally, the methods used to investigate the intrinsic traits of O157:H7 (serological methods, cell culture, and biochemical reactions (Lebeis et al., 2008; Bonetta et al., 2011)) cannot reflect the true virulence of O157:H7 because O157:H7 expresses its full virulence only after coming into contact with the host cells and activating the corresponding signaling pathway. For example, the type III secretory system is closely associated with pathogenicity (Bonyadian et al., 2010). However, this system can only be activated after O157:H7 contacts the host cells. In short, the current, universally adopted methods for O157:H7 virulence assessment neglect the direct infection of host cells by O157:H7 and their effects such as infection triggers, fail to investigate the interactive effects of O157:H7 and the host cells, and fail to comprehensively and accurately reflect the true pathogenicity of O157:H7.

The composition of O157:H7 virulence factors is complex and still not fully understood, and the consolidated results obtained from employing different analytical methods allow a more comprehensive understanding of the virulence of O157:H7. Therefore, a comprehensive analysis of the effect of cell damage caused by O157:H7 is necessary. The objective of our study is to find some more sensitive, accurate, and quantifiable methods for the systematic virulence assessment of O157:H7 and techniques for pathogenicity analysis. In this study, we found three different methods, flow cytometry and cell vitality and LDH release analyses and fluorescence detection, which were supplementary to yield standard operating procedures for the analysis of cytotoxicity in O157:H7.

2. Materials and methods

2.1. Bacterial isolates and culture

The *E. coli* O157:H7 strain EDL933 (*stx*1-, *stx*2-, *eaeA*-, *ehxA*-, *tccp*- and *espA*-positive) was originally isolated from a patient with diarrhea (Riley et al., 1983) and was kindly provided by Prof. Long Liang (Institute of Biotechnology, Beijing). A CT-Sorbitol MacConkey agar plate (CT-SMAC) was used as a selective medium for the isolation and differentiation of O157:H7. The K-12 strain *E. coli* MG1655, a human commensal strain, was obtained from ATCC. The original *E. coli* strain K-12 was obtained from a stool sample of a diphtheria patient in Palo Alto, CA in 1922 (Neidhardt and Curtiss, 1996).

Bacterial cultures were propagated in Luria-Bertani agar or grown aerobically with constant shaking (200 rpm) in Luria-Bertani broth at 37 °C. The number of *E. coli* O157:H7 or K-12 cells was determined by the drop-plate method. Briefly, 0.1 ml of each sample was spread onto three Luria-Bertani agar plates, which were then incubated at 37 °C for 15 h.

2.2. Cell culture

Cells of the human epithelial cell lines HeLa and HT-29 were cultured in DMEM (Dulbecco's Modified Eagle Medium) and RPMI (Roswell Park Memorial Institute) 1640 media, respectively, with the addition of 10% fetal bovine serum (FBS). The cells were incubated at 37 °C in 5% CO_2 in a humidified incubator. Cells were plated 18 to 24 h prior to infection so that the cell density reached 90% confluency at the time of infection. For fluorescence microscopy, cells were grown on coverslips.

2.3. Infection conditions

O157:H7 and K-12 were grown overnight with constant shaking (200 rpm) at 37 °C in Luria-Bertani broth. Then, they were diluted with fresh broth and cultured until the mid-logarithmic phase of growth ($OD_{600} = 0.3$). Bacteria were harvested, washed with phosphate buffered saline (PBS), resuspended in fresh cell culture medium with 5% FBS and adjusted to the appropriate density.

2.4. Flow cytometry assay

The supernatants of the infected cultures were removed to preserve the detached cells. Subsequently, the adherent cells were harvested by standard trypsin treatment and combined with the cells from the supernatants. Cell samples were washed once with PBS and submitted to analysis by flow cytometry. Cell apoptosis was analyzed using the PE Annexin V Apoptosis Detection Kit I(BD, USA). Uninfected cells served as a negative control to set the threshold marker for the discrimination of fluorescein isothiocyanate (FITC)-negative and -positive cells. According to the manufacturer's instructions, cells that are considered viable are PE Annexin V and 7-Amino-Actinomycin (7-AAD) negative; cells that are in early apoptosis are PE Annexin V positive and 7-AAD negative; and cells that are in late apoptosis or already dead are both PE Annexin V and 7-AAD positive.

2.5. Lactate dehydrogenase (LDH) assay

After infection with O157:H7 or K-12, LDH was assayed using a Cytotox 96 Non-Radioactive Cytotoxicity Assay kit (Promega, Madison, WI, USA). Fifty microliters of the supernatant from each culture were transferred to a 96-well plate. For maximum LDH release, cell lysis solution was added to each well, followed by 50 μl of the reconstituted substrate mix. After stopping the reaction, the absorbance was measured at

490 nm using an enzyme-linked immunosorbent assay (ELISA) reader. Untreated cells were lysed with 10 μl of 10% Triton-X100 in water (Millipore) as a positive control. The proportion of dead cells in each well (cytotoxicity) was calculated as [(experimental − target spontaneous) / (target maximum − target spontaneous)] × 100.

2.6. CellTiter-fluor™ cell viability assay

Cell viability was analyzed using CellTiter-Fluor cell viability assays (Promega, Madison, WI, USA). HeLa and HT-29 cells were seeded in 96-well culture plates, and following overnight incubation, the cells were infected with O157:H7 and K-12 at defined multiplicity of infection (Garg et al., 2008) ratios. CellTiter-Fluor reagent was added to measure cell viability after 6 h post-infection, and the absorbance at 490 nm determined following 30 min of incubation using plate reader (Versa max, Molecular Devices) according to the manufacturer's instructions. The mean of six experimental replicates from three independent experiments was determined. Untreated HeLa and HT-29 cells served as vehicle control. Cell viabilities were calculated as percentages of the vehicle control. Statistical analysis was carried out using Student's t-test.

2.7. Fluorescence detection

HeLa cells infected with O157:H7 (MOI = 800:1) and K-12 (MOI = 800:1) were seeded onto sterile coverslips, washed with PBS, and fixed in 4% paraformaldehyde (PFA) for 20 min at room temperature (RT). After washing and permeabilizing the cells with 0.2% Triton X-100 for 10 min at RT, cells were incubated with TRITC-conjugated phalloidin (Millipore, Billerica, USA) for 30 min at RT and stained with 0.2% DAPI solution, with washes between each step. The cells were examined using a Nikon Eclipse TE2000-U fluorescence microscope.

2.8. Statistical analysis

The significance of variability between the means of the experimental groups was analyzed by Student's t-test with the Satterthwaite approximation.

$$t' = \frac{\overline{X}_1 - \overline{X}_2}{\sqrt{\frac{S_1^2}{n_1} + \frac{S_2^2}{n_2}}} \qquad v = \frac{\left(S_{\overline{X}_1}^2 + S_{\overline{X}_2}^2\right)^2}{\frac{S_{\overline{X}_1}^4}{n_1 - 1} + \frac{S_{\overline{X}_2}^4}{n_2 - 1}}$$

All data are presented as mean ± SD. Two paired Student's t-test was performed to determine significance at $p < 0.05$(*), $p < 0.01$(**), $p < 0.001$(***).

3. Results

To assess the cytotoxicity of O157:H7, *E. coli* strain K-12 (a non-EHEC strain) was selected as the control. We investigated cytomorphology, adhesion, apoptosis, cell viability, and the enzymatic activity of living epithelial cells post-infection, as well as the cytotoxicity of O157:H7 to epithelial cells with respect to cell membrane integrity.

3.1. Cellular apoptosis assays by flow cytometry

To investigate the cytotoxicity effects of O157:H7 more comprehensively, we first used cellular apoptosis assays to monitor host cell apoptosis in a time-dependent manner. Flow cytometry is important for measuring cellular apoptosis. In this study, we used flow cytometry to analyze the difference in the progress of cellular apoptosis after HeLa cells were infected with O157:H7 and K-12, respectively.

HeLa cells were infected with O157:H7 or K-12, with a MOI of 800:1 (Garg et al., 2008). After 2 h to 7 h post-infection, cells were harvested and labeled with fluorescein isothiocyanate (FITC) as described previously. As shown in Fig. 1, most cells began to show apoptosis at 3 h post-infection with O157:H7. The number of apoptotic cells was rapidly increasing at 4 h post-infection with O157:H7. Together, these results indicate that O157:H7 caused more serious injury to the cells than did K-12, and there was a pronounced difference in cytotoxicity between O157:H7 and K-12. These findings demonstrate that this assay can accurately reveal differences in the cytotoxicity of different strains.

3.2. Cell viability assay and LDH assay

After host cells were infected with O157:H7, the cell membrane structure was damaged through multiple virulence factors, causing an overall increase in the permeability of the cell membrane and the release of cytosolic contents. Therefore, we measured the intracellular constituents to assess cell membrane integrity and permeability.

Our first protocol measured the intracellular molecules that serve as viability markers. Here, we investigated the change in the distribution of enzymatic activity within the cells. As a living cell marker, the live-cell protease is only active in cells that have a healthy cell membrane (Niles et al., 2007), indicating cell viability. This assay is a widely adopted standard method for measuring cell membrane integrity. The integrity of the cell membrane can be determined through intracellular changes in enzymatic activity.

We measured the intracellular enzymatic activity after infection with O157:H7 (MOI = 16:1) or K-12 (MOI = 16:1). As shown in Fig. 2, O157:H7 caused more serious cell damage than K-12. In addition, lower cell viability was observed post-infection with either O157:H7 or K-12; however, at corresponding time points, the activity of HeLa cells infected with O157:H7 was lower than that infected with K-12. Similarly, the activity of HT-29 cells infected with O157:H7 was lower than that of cells infected with K-12 at the same time point. O157:H7 had an obvious influence on the viability of HeLa and HT-29 cells; this result indicates that the cytotoxicity of O157:H7 can be quantitatively measured. The cell viability assay can accurately reveal the different cytotoxicity levels of different strains. Whereas after infected with O157:H7 or K-12, the differences of HT-29 cell variability were more obvious than the viability of HeLa. At 4.5 h and 6 h post-infection of O157:H7 or K-12, the viability of HeLa had no significant difference, while the viability of HT-29 had significant difference. We can conclude that HT-29 cell could be used more sensitively to differentiate the differences of virulence between different bacterial strains by this method.

As a supplement to the method described above, we considered it important to detect not only the residual amounts of critical molecules after host cell infection with the bacteria but also the release of intracellular material. LDH is a stable cytoplasmic enzyme present in all cells. It is rapidly released into the cell culture supernatant when the plasma membrane is damaged.

To determine the cytotoxicity effect of O157:H7 in epithelial and intestinal cells, we measured the level of LDH in the supernatants post-infection. The level of LDH increased significantly with the time-dependent and MOI dose-dependent increase in cytotoxicity in O157:H7-infected HeLa cells compared with the level of LDH in K-12-infected cells (Fig. 3A and C). Furthermore, these results were replicated in the LDH analyses of infected HT-29 cells (Fig. 3B and D).

As shown in Fig. 3, we analyzed the cytotoxicity of different doses of bacteria to HeLa and HT-29 cells at 3 h post-infection with O157:H7 and K-12, and we also analyzed the cytotoxicity of O157:H7 and K-12 under a fixed infectious dose (MOI = 16:1) to HeLa and HT-29 cells. With increasing dose, the toxicity of both O157:H7 and K-12 to HeLa and HT-29 cells increased (Fig. 3A and B); however, at the same dose, the cytotoxicity of O157:H7 was stronger than that of K-12 to both HeLa and HT-29 cells, indicating that the different bacteria had different levels of cytotoxicity to HeLa and HT-29 cells. Thus, the virulence of the different strains of O157:H7 can be assessed by this method. Meanwhile, at the fixed dose (MOI = 16:1) (Fig. 3C and D), the cytotoxicity of O157:H7

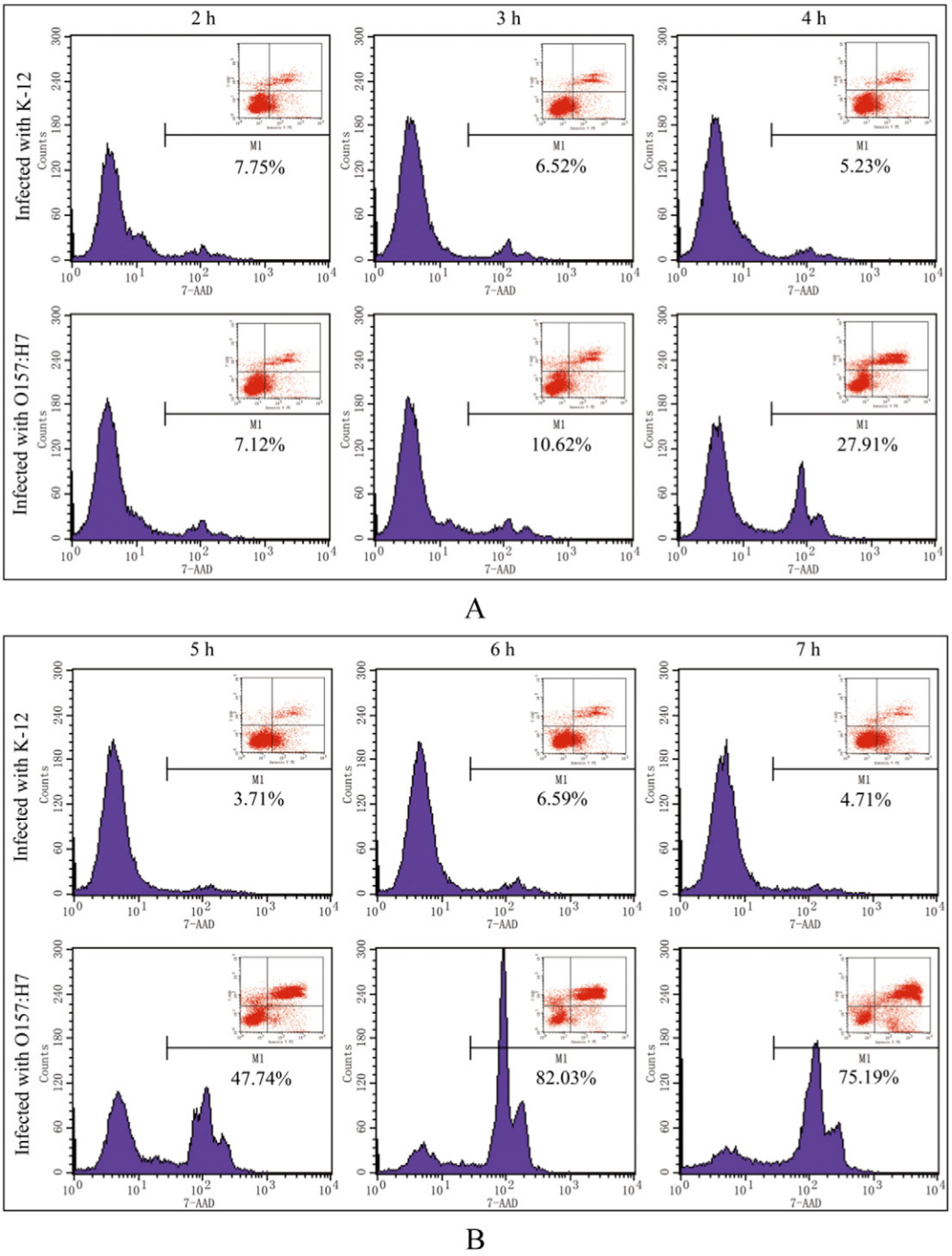

Fig. 1. Flow cytometry assay of apoptosis of epithelial cells after infection with K-12, a non-EHEC strain, or O157:H7. HeLa cells were infected with O157:H7 and K-12 at a MOI of 800:1. The infected cells were harvested and labeled with FITC, and the percentages of FITC-positive cells were determined by flow cytometry at 2 h, 3 h, 4 h, 5 h, 6 h, and 7 h post-infection.

and K-12 to HeLa and HT-29 cells increased over time, but at any single time point, the two strains had different cytotoxicity levels; this procedure may therefore be used to quantify the cytotoxicity of different strains of O157:H7. Meanwhile we noticed that, in Fig. 3A, between the variability of HeLa cell assays, the point where 16:1 MOI is used for 3 hours there had no significant difference. However, in panel C, using 16:1 MOI between 2 and 4 h, there is >50% difference (indicated to be significant). Compared with HT-29 cells, Hela cells were not very sensitive, and the results were unstable, so HT-29 cells were more appropriate as detecting cells by this method.

3.3. Fluorescence

Bacteria effect protein, EspFu, can induce the formation of actin pedestals, which is needed by bacteria adhesion. Bacteria adhesion is related to bacteria infectivity, which is a part of the cytotoxicity of bacteria. So through detecting the formation of actin pedestals, the cytotoxicity of *E. coli* O157:H7 can be observed. After the host cells were infected with O157:H7, the cytomorphology of the cells changed. As shown in Fig. 4, fluorescence was used to observe the host cells after bacterial infection and to monitor changes in the distributions of the cytoskeleton molecule actin and Vinculin. The figure shows the distribution of

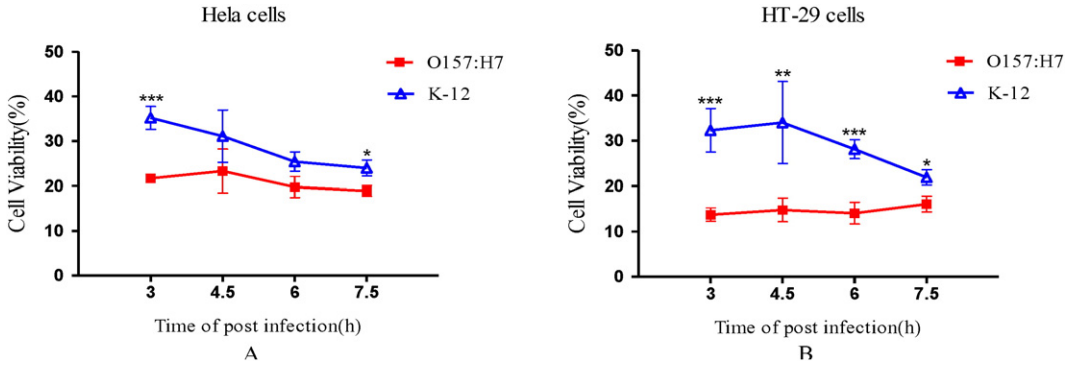

Fig. 2. Time-dependent effects on cell viability of HeLa cells (A) and HT-29 cells (B) after infection with *E. coli* O157:H7 (MOI = 16:1) and K-12 (MOI = 16:1). From 3–7.5 h post-infection, the viability of HeLa cells infected with O157:H7 decreased faster than infected HT-29 cells. The viability of HeLa cells infected with O157:H7 was lower than that of cells infected with K-12 in HeLa and HT-29 cells at corresponding time points (*, $p < 0.05$; **, $p < 0.01$; ***, $p < 0.001$).

fluorescence in HeLa cells at 3 h or 6 h post-infection with O157:H7 and K-12, respectively. Red fluorescence on the membranes of HeLa cells indicates the distribution of actin. Brighter areas of red fluorescence on the cell membrane represent more concentrated areas of actin. In addition, green fluorescence on the membranes of HeLa cells indicates Vinculin. The molecular configuration of the cytoskeleton actin on the cell membrane underwent a significant change post-infection. However, infection with O157:H7 produced a more significant change in cytoskeletal structure than did infection with K-12. This result demonstrates the characteristic cytological effects of O157:H7 and shows that monitoring changes in cytoskeletal structure can be used to assess the cytological effects of O157:H7.

4. Discussion

O157:H7 infection has become an important public health problem threatening populations around the world (Lynch et al., 2006). O157:H7 is highly pathogenic, and the use of antibiotic treatment can aggravate O157:H7 infections (Bielaszewska et al., 2011). Currently, there are no effective treatments for the disease; therefore, preventing O157:H7 infection is particularly important. If we can comprehensively and accurately assess the virulence of O157:H7 clinical isolates, then we can provide reliable data for clinical disease prevention and a method for the pre-assessment of newly discovered O157:H7 epidemics.

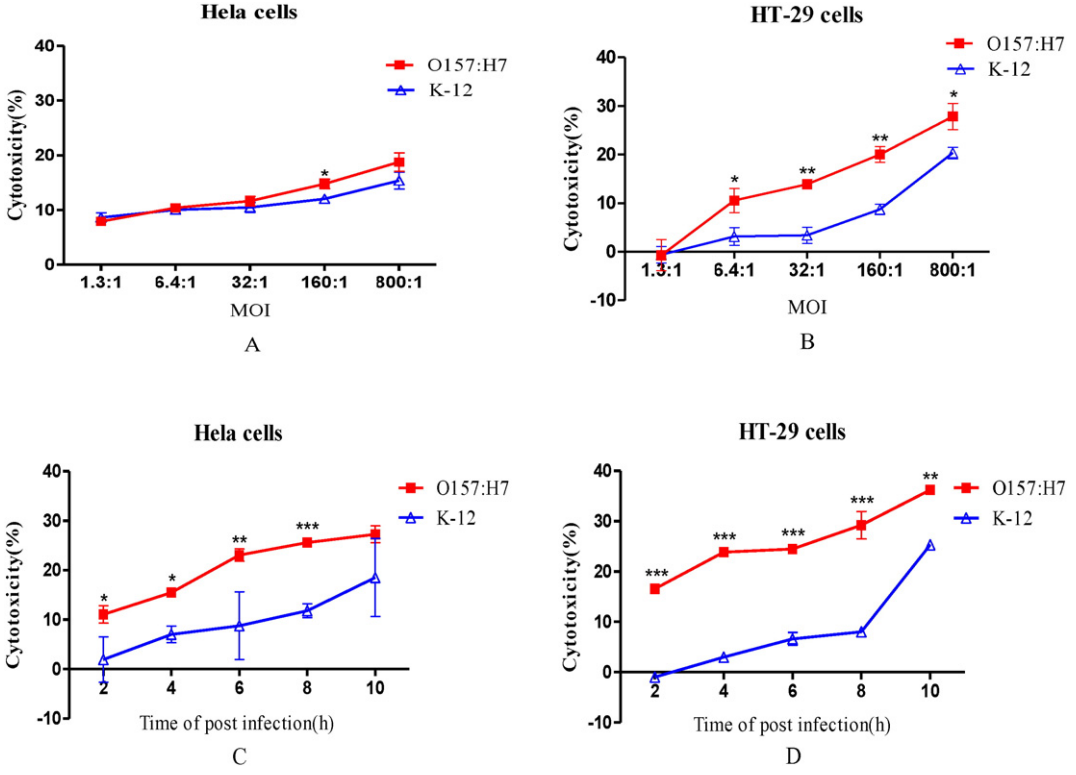

Fig. 3. Dose- and time-dependent effect of cell cytotoxicity of *E. coli* O157:H7 and K-12. HeLa and HT-29 cells were infected as described in the Materials and Methods section. A and B show the cytotoxicity to HeLa and HT-29 cells infected by O157:H7 or K-12 at various doses (MOI = 1.3:1–800:1) at 3 h post-infection, and the increasing trend of the curves is consistent with the increase in infectious doses of O157:H7 and K-12 (A and B). Toxicity of O157:H7 and K-12 to HeLa and HT-29 cells increased with increasing duration of infection with O157:H7 and K-12, and after the first time point (2 h), the cytotoxicity of O157:H7 was significantly higher than that of K-12 (*, $p < 0.05$; **, $p < 0.01$; ***, $p < 0.001$). Meanwhile, under the fixed infectious dose, MOI = 16:1, cytotoxicity increased over time (C and D). Furthermore, at corresponding time points, the cytotoxicity of O157:H7 to either the HeLa or HT-29 cells was greater than the cytotoxicity of K-12.

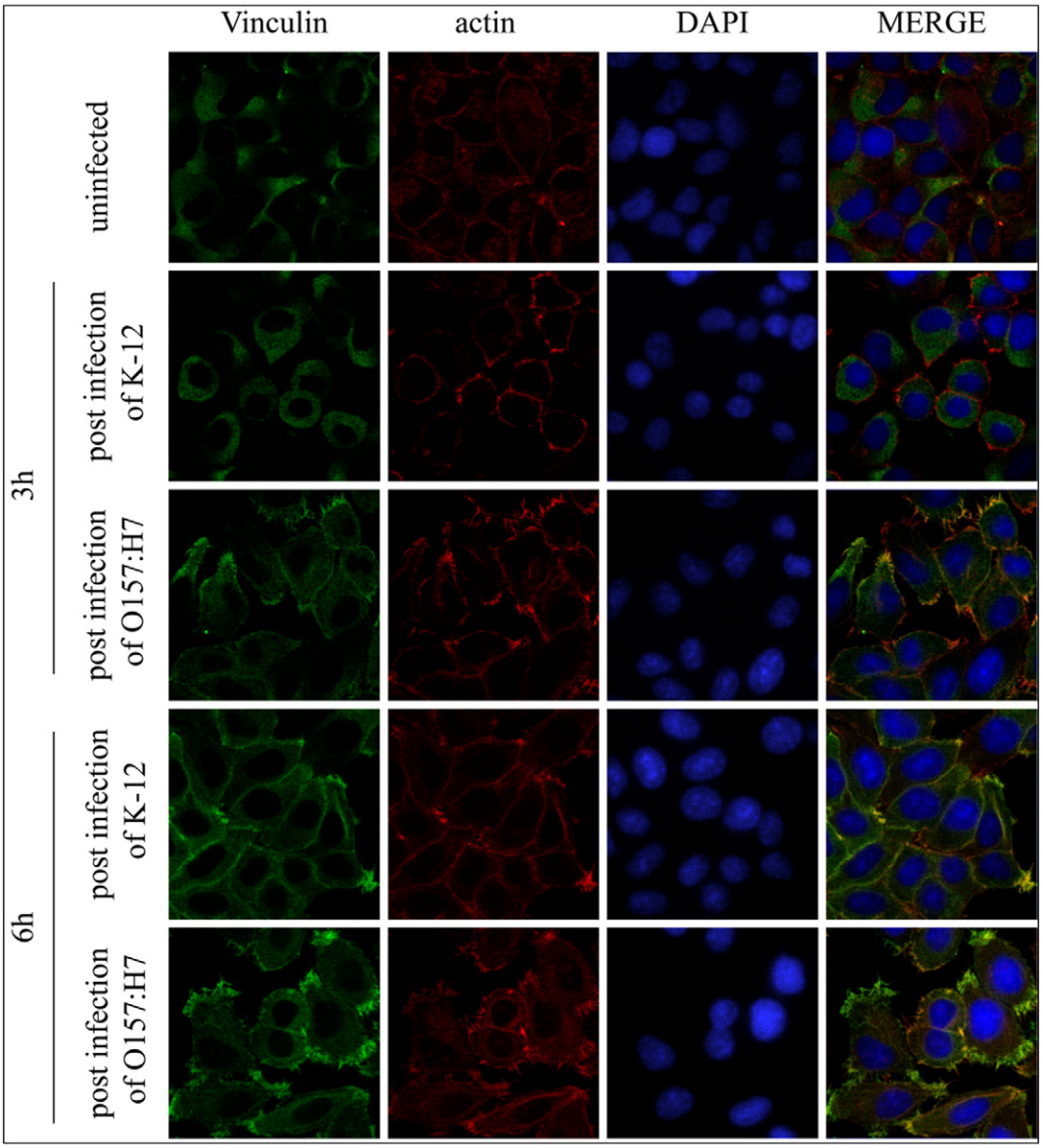

Fig. 4. The distribution of actin in HeLa cells detected by the fluorescence method. F-actin was detected using TRITC-conjugated phalloidin (Millipore, Billerica, MA, USA). Red fluorescence on the membranes of HeLa cells indicates actin, and green fluorescence on the membranes of HeLa cells indicates Vinculin. Nuclear counterstaining was revealed with DAPI, and all images were overlaid.

Because the composition of O157:H7 virulence factors is complex and still not fully understood, the consolidated results obtained from employing different analytical methods allow a more comprehensive understanding of the virulence of O157:H7. In the present study, we focused on the differences in the damaging effects observed between host cells infected with either O157:H7 or K-12. We performed three supplementary methods for assessing the overall state of the host: i) flow cytometry to quantitatively analyze the progress of apoptosis of infected host cells, thus characterizing the cytotoxicity of O157:H7 to the host cells; ii) cell vitality and LDH release analyses to quantitatively measure the loss of cell membrane integrity of infected cells, thus characterizing the toxicity of O157:H7 to the host cells; and iii) fluorescence detection to observe changes in the distribution of actin and the skeletal structure of the cell membranes of infected cells, thus characterizing the influence of O157:H7 on the host cells in an intuitive manner.

The first assay enables the quantitative analysis of the progression of host cell apoptosis resulting from multiple O157:H7 virulence factors and thus assesses virulence of O157:H7 in a comprehensive manner. This method requires a flow cytometer to conduct the assay. The second assay quantitatively analyzes the degree of damage suffered by the cell membranes of infected host cells and is used to assess the effects of damage to the cell membranes during infection with O157:H7. This method can simultaneously measure multiple specimens. For the assay, 96-, 384-, or 1536-well opaque-walled tissue culture plates can be used. Thus, this method enables high-throughput sampling and analyses. The third assay detects changes in cytomorphology that occur in the host cell skeleton post-infection with O157:H7. This method, performed by direct observation, can differentiate the virulence of different bacterial strains. For the cytomorphological analysis, the readout can be quantified through many means. It is relative quantification. For example, fluorescence signals can be analyzed using a Leica DM4000B microscope equipped with appropriate filters and a DFC300FX camera under the control of LAS V4.0 software (Leica). But we have not done this work in this study. This difference can also be observable through visual inspection, roughly.

The simultaneous adoption of these three supplementary methods can be regarded as an effective supplement to the standard protocols for testing virulence of O157:H7, due to its comprehensive, accurate,

and quantitative nature. In addition, our study provides an important reference for accurately assessing the pathogenicity of O157:H7 clinical isolates. The methods described here have wide applicability. They can be applied to analyze the virulence of not only O157:H7 but also other classes of pathogenic bacteria.

Concluding remarks

The three methods can more comprehensively analyze O157:H7 cytotoxicity than the traditional methods, and the cytotoxicity of pathogenic bacteria was more directly and clearly observed through them, so they are more sensitive, accurate, and quantifiable method for the systematic virulence assessment of O157:H7.

Because the composition of virulence factors of O157:H7 is very complex and not fully understood, the comprehensive and accurate measurement of the cytotoxicity of O157:H7 can provide a deeper understanding of virulence and be used for the pre-assessment of emerging O157:H7 outbreaks.

This study established three supplementary methods for measuring different aspects of O157:H7-induced damage to human epithelial cell lines. The three methods place particular emphasis on the interaction between O157:H7 and host cells as well as the changes O157:H7 induces in host cells.

The simultaneous adoption of these three methods will enable the cytotoxicity assessment of O157:H7 and similar strains in a comprehensive, accurate, and quantitative manner. These methods can also be applied to other pathogenic bacteria with cytotoxic activity to host cells.

Acknowledgments

This work was supported by the National Natural Science Foundation of China (81000763) and the National Basic Research Program of China (973 Program) 9732009CB52604. *E. coli* O157:H7 strain EDL933 was kindly provided by Prof. Long Liang (Institute of Biotechnology, Beijing).

References

Badouei, M.A., et al., 2010. Virulence gene profiles and intimin subtypes of Shiga toxin-producing *Escherichia coli* isolated from healthy and diarrhoeic calves. Vet. Rec. 167 (22), 858–861.

Beltz, L.A., 2011. Emerging infectious diseases: a guide to diseases, causative agents, and surveillance. Public health/epidemiology and biostatistics, 1st ed. Jossey-Bass, San Francisco (xvi, 734 p.).

Bielaszewska, M., et al., 2011. Chromosomal instability in enterohaemorrhagic *Escherichia coli* O157:H7: impact on adherence, tellurite resistance and colony phenotype. Mol. Microbiol. 79 (4), 1024–1044.

Bonetta, S., et al., 2011. Development of a PCR protocol for the detection of *Escherichia coli* O157:H7 and *Salmonella* spp. in surface water. Environ. Monit. Assess. 177 (1–4), 493–503.

Bonyadian, M., et al., 2010. Identification & characterization of Shiga toxin-producing *Escherichia coli* isolates from patients with diarrhoea in Iran. Indian J. Med. Res. 132, 328–331.

Byelashov, O.A., et al., 2010. Evaluation of brining ingredients and antimicrobials for effects on thermal destruction of *Escherichia coli* O157:H7 in a meat model system. J. Food Sci. 75 (4), M209–M217.

Dziva, F., et al., 2007. EspP, a Type V-secreted serine protease of enterohaemorrhagic *Escherichia coli* O157:H7, influences intestinal colonization of calves and adherence to bovine primary intestinal epithelial cells. FEMS Microbiol. Lett. 271 (2), 258–264.

Garg, A.X., et al., 2008. Albuminuria and estimated GFR 5 years after *Escherichia coli* O157 hemolytic uremic syndrome: An update. Am. J. Kidney Dis. 51 (3), 435–444.

Hayashi, T., et al., 2001. Complete genome sequence of enterohemorrhagic *Escherichia coli* O157:H7 and genomic comparison with a laboratory strain K-12. DNA Res. 8 (1), 11–22.

Kauffman, M.D., LeJeune, J., 2011. European Starlings (*Sturnus vulgaris*) challenged with *Escherichia coli* O157 can carry and transmit the human pathogen to cattle. Lett. Appl. Microbiol. 53 (6), 596–601.

Lebeis, S.L., Sherman, M.A., Kalman, D., 2008. Protective and destructive innate immune responses to enteropathogenic *Escherichia coli* and related A/E pathogens. Future Microbiol 3 (3), 315–328.

Lim, J.Y., Yoon, J., Hovde, C.J., 2010. A brief overview of *Escherichia coli* O157:H7 and its plasmid O157. J. Microbiol. Biotechnol. 20 (1), 5–14.

Lynch, M., et al., 2006. Surveillance for foodborne-disease outbreaks—United States, 1998–2002. MMWR Surveill. Summ. 55 (10), 1–42.

Mead, P.S., Griffin, P.M., 1998. *Escherichia coli* O157: H7. Lancet 352 (9135), 1207–1212.

Moxley, R.A., 2004. *Escherichia coli* 0157:H7: an update on intestinal colonization and virulence mechanisms. Anim. Health Res. Rev. 5 (1), 15–33.

Neidhardt, F.C., Curtiss, R., 1996. *Escherichia coli* and *Salmonella*: cellular and molecular biology. 2nd ed. ASM Press, Washington, D.C.

Niles, A.L., et al., 2007. A homogeneous assay to measure live and dead cells in the same sample by detecting different protease markers. Anal. Biochem. 366 (2), 197–206.

Perna, N.T., et al., 2001. Genome sequence of enterohaemorrhagic *Escherichia coli* O157: H7. Nature 410 (6825), 240 (vol 409, pg 529, 2001).

Riley, L.W., et al., 1983. Hemorrhagic colitis associated with a rare *Escherichia coli* serotype. N. Engl. J. Med. 308 (12), 681–685.

Shabanova, N.A., et al., 2009. [Influence of *Lactobacillus fermentum* metabolites on ultrastructure of pathogenic *Escherichia coli*]. Zh. Mikrobiol. Epidemiol. Immunobiol. 2, 3–6.

Strockbine, N.A., et al., 1986. Two toxin-converting phages from *Escherichia coli* O157:H7 strain 933 encode antigenically distinct toxins with similar biologic activities. Infect. Immun. 53 (1), 135–140.

Wang, P., et al., 2011. pO157_Sal, a novel conjugative plasmid detected in outbreak isolates of *Escherichia coli* O157:H7. J. Clin. Microbiol. 49 (4), 1594–1597.

Wong, A.R.C., et al., 2011. Enteropathogenic and enterohaemorrhagic *Escherichia coli*: even more subversive elements. Mol. Microbiol. 80 (6), 1420–1438.